An automatic procedure to retrieve the windfields from SAR Images

Stefano Zecchetto[1] and Paolo Trivero[2]

[1]Istituto di Scienze dell'Atmosfera e del Clima, CNR, Padova, Italy
[2]Dipartimento di Scienze e Tecnologie Avanzate, Università di Alessandria, Alessandria, Italy
E-mail: s.zecchetto@isac.cnr.it

Abstract
This paper describes an automatic procedure to download and process SAR images in the coastal areas, in order to get the wind field. The images processed are the Envisat ASARWide Swath. The methodology to retrieve b the wind fields is based on the 2-D Continuous Wavelet Transform, developed in Zecchetto and De Biasio [2002] and applied in Zecchetto and De Biasio [2008]. About three images per day are processed since May 2008. Co-location of the SAR derived winds with those provided by QuikSCAT and Metop will permit to validate the methodology over a large variety of atmospheric regimes. Once validation will be accomplished, the procedure described in this paper will be used to derive the wind fields for coastal meteorology applications.
Keywords: SAR, wavelet, MABL, sea wind.

Una procedura automatica per derivare il campo del vento da immagini SAR

Riassunto
Il presente lavoro descrive una procedura automatica di downloading e processamento di immagini Envisat ASAR Wide Swath sviluppata per stimare il campo del vento. La metodologia utilizzata si basa sulla trasformata wavelet in due dimensioni, sviluppata ed utilizzata in Zecchetto and De Biasio [2002, 2008]. Nell'area d'interesse si ottengono circa tre immagini al giorno. Alle immagini processate sono associati i venti misurati dagli scatterometri dai satelliti QuikSCAT e Metop. Tale co-locazione permetterà di validare il metodo utilizzato per la stima del vento. Quando la validazione sarà terminata, la procedura descritta nel presente lavoro sarà utilizzata per applicazioni di meteorologia costiera.
Parole chiave: *SAR, wavelet, MABL, vento*.

Introduction
In this paper we describe an automatic procedure to download and process the Envisat Wide Swath SAR Images, in order to estimate the wind field over the imaged sea areas. Once converted in backscatter Normalized Radar Cross Section units, the images are analyzed

by the two dimensional Continuous Wavelet Transform (CWT2), which permits to isolate the SAR backscatter structures linked to the structure of the Marine Atmospheric Boundary Layer (MABL), and then to extract the wind direction and speed.
The paper is structured as follows: section 2 illustrate the procedure to get and process the SAR images, while section 3 outlines the basic concepts of the two dimensional continuous wavelet transform and the methodology for wind extraction. Section 4 provides the conclusions.

The procedure to download and process ASAR Wide Swath images

The ASAR Wide Swath images

The Envisat images used here are the ASAR Wide Swath [ESA, 2002]. They are about 400 km wide but cover areas of different sizes, depending on the swath length. Their pixel size is of 75 m by 75 m.

The procedure

The whole procedure run under *Linux* using bash scripts.
The ASAR Wide Swath images are downloaded from the *ftp* site
`oa-es.eo.esa.int` and the web site
`http://oa-ip.eo.esa.int/ra/asa`, made available by ESA in the framework of the project C1P.5404.

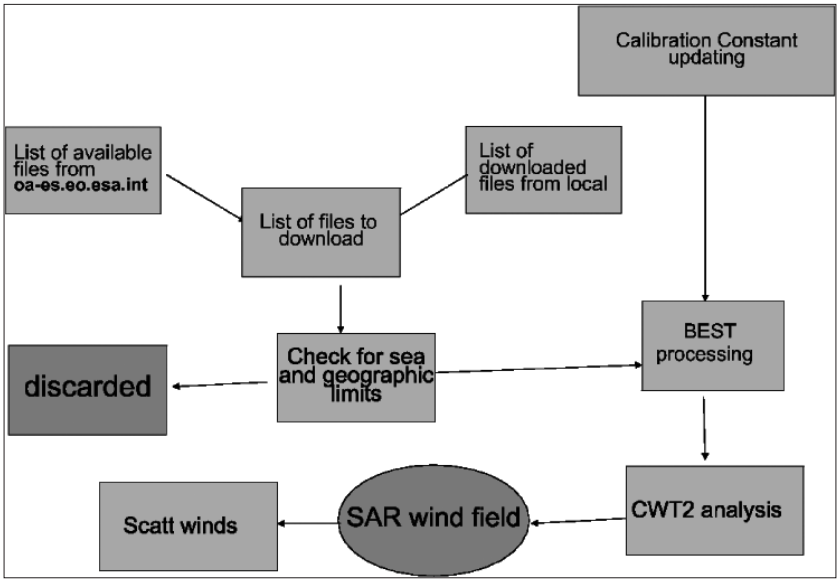

Figure 1 - The flow chart of the automatic downloading and processing.

Figure 1 shows the flow chart of the procedure, which starts with the possible updating of the External Calibration constant through the download of the ESA generated External Calibration File on

http://earth.esa.int/services/auxiliary_data/asar
and the automatic creation of a *ini* file to be processed with BEST software [ESA/Esrin and Telespazio, 2006]. This permits to process the SAR images with the most updated calibration constant and thus to get the most calibrated image in cross section linear units. The second step is to list the available images on the *ftp* and *web servers*. Comparing such a list with that of the files already downloaded, to avoid to download the same images twice, a list of the new files to download is created. On each downloaded image, a check is carried out to verify if it lies inside the area of interest and if so, if the imaged scene contains at least the 40% of sea. This check successful, the image goes to a basic processing via BEST, otherwise it is discarded. BEST processing yields the image in linear cross section units, along with the ancillary files needed for further processing, consisting on the image analysis with a method based on the two dimensional Continuous Wavelet Transform (CWT2) Zecchetto and De Biasio [2008], illustrated in the next section. After CWT2, a search is performed about the available satellite scatterometer winds covering the scene, downloaded in Near Real Time from the *KNMI ftp server* in the framework of the Ocean & Sea Ice Satellite Application Facility (www.osi-saf.org) of EUMETSAT (www.eumetsat.org). Satellite wind data originate from the NASA *QuikSCAT* [JPL, 2001] and the Eumetsat *Metop* [SAF, 2007].

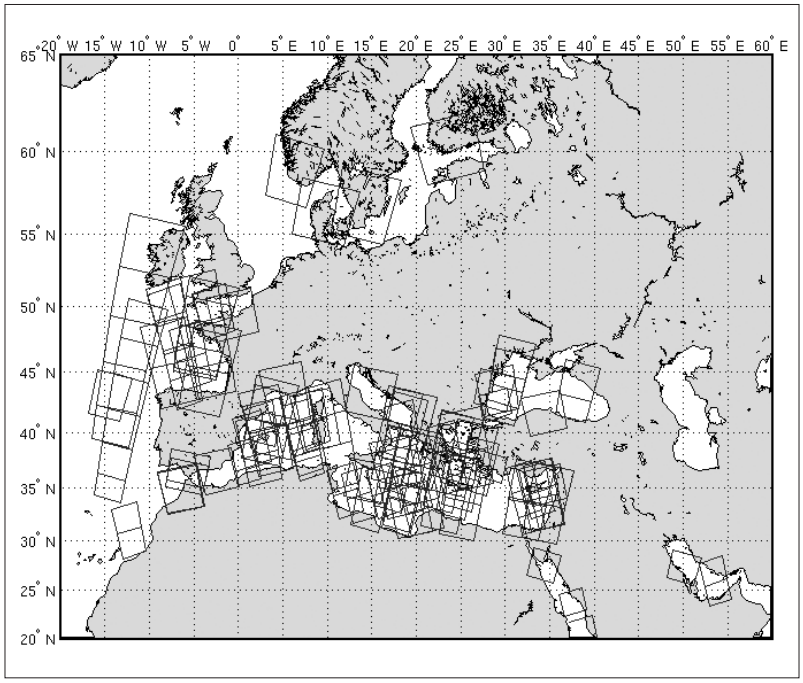

Figure 2 - The ASAR frames acquired and processed from 1 January to 30 April 2009.

This procedure is continued until all the available new ASAR files have been downloaded and checked, and then repeated several times per day looking for new images. Since

the original ASAR images may consist of large swathes, they have been cut into frames characterized by the same number of rows and columns. Thus a frame covers about a 400 km by 400 km area.
The area of interest has been set as 20 W to 60 E and 10 N to 65 N. The procedure started on May 2008, downloading and processing about three ASAR frames per day: the location of the ASAR frames acquired from 1 January to 30 April 2009 is reported in Figure 2.

The methodology of wind extraction

The methodology of wind extraction is explained in details in Zecchetto and De Biasio [2002, 2008]. Its essential steps are:

- image preprocessing, to let the image suitable to CWT2 analysis;
- choice of the CWT2 scales of processing;
- CWT2 of the image;
- wavelet variance map, to get the scales of maximum energy;
- reconstruction of the image using only the scales of maximum energy, to isolate the backscatter cells;
- choice of the aliased direction;
- dealiasing the wind directions;
- the wind speed computation.

The Continuous Wavelet Transform (CWT) [Beylkin et al., 1992; Kaiser, 1994; Foufoula-Georgiou and Kumar, 1994; Antoine and Murenzi, 2004] $\tilde{f}$ of a function *f(u)*is a local transform, dependent on the parameters s and τ, defined as

$$\tilde{\mathrm{f}}(s,\tau) = \langle \psi_{(s,\tau)}, f \rangle = \int_{-\infty}^{+\infty} du \psi^{*}_{(s,\tau)}(u) f(u) \quad [1]$$

where $\psi_{(s,\tau)}(u) = |s|^{-1} \psi\left(\frac{u-\tau}{s}\right)$ is the mother wavelet at a given scale (or dilation) s and location τ. The asterisk denotes complex conjugation. The quantity $\left|\tilde{\mathrm{f}}(s,\tau)\right|^2$ plays the role of local energy density at given (s,τ). In two dimensions,

$$\tilde{\mathrm{f}}(s_x,\tau_x;s_y,\tau_y) = \iint_{-\infty}^{+\infty} du\, d\upsilon \psi^{*}_{(s_x,\tau_x)}(u) \quad [2]$$
$$\psi^{*}_{(s_y,\tau_y)}(\upsilon)\, f(u,\upsilon)$$

Equation [2] has been computed using the Mexican Hat mother wavelet. It has the property of capturing the fine scale structure of the data, and is suitable for the continuous wavelet transform because it is non-orthogonal [Torrence and Compo, 1998]. The SAR images have been compressed by a factor two: this filters out geophysical phenomena at scales shorter than 150 m as, for instance, sea gravity waves, without hiding the backscatter structures related to the atmosphere dynamics. The images have to be preprocessed before the CWT2 analysis, to mask the land and to mitigate the effects introduced by the variation in range of the radar incidence angle. The incidence angle mitigation, performed by an high pass filter with a cutoff length 0 f 40 km, is needed to avoid that structures on the inner part of the image, where the radar incidence angle is smaller and the radar backscatter

higher, prevail on the outer ones. The resulting image is not anymore expressed in absolute backscatter values: the important fact is that locally the ASAR features are maintained. A more detailed explanation of the ASAR pre-processing may be found in Zecchetto and De Biasio [2008].
The scales range is very important because it defines the geophysical phenomena to study: we focus on the spatial range from 300 m to 4 km. The scales (s_r,s_c) have been obtained dividing logarithmically the range of interest in 8 intervals, thus producing 64 maps for each SAR image. The CWT2 yields the wavelet coefficients used to compute the wavelet variance map, which provides information about the energy distribution as a function of (s_r,s_c), in the same way as the two dimensional Fourier spectrum does as a function of wavenumbers. The scales for the image reconstruction are taken around the maximum of the wavelet variance map often, but not always, well defined.

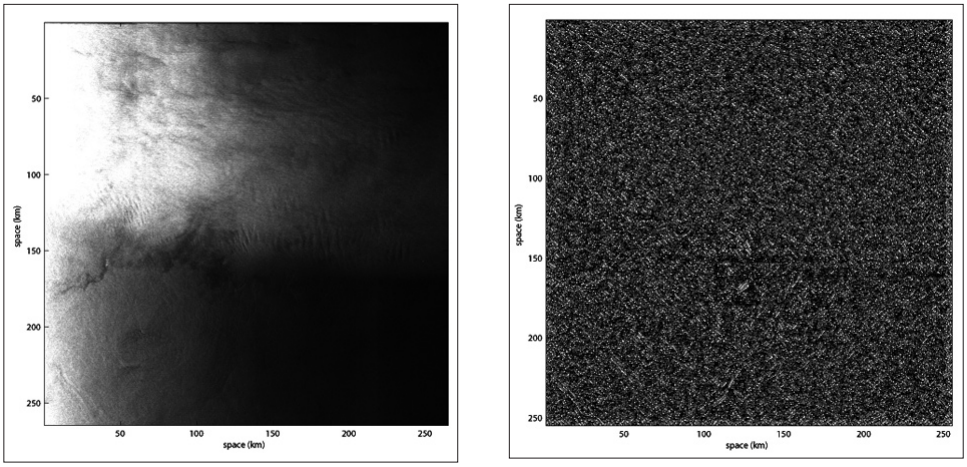

Figure 3 - Left panel: an ASAR WS image processed: 20-JUN-2008 at 22:26:47 GMT. Right panel: the reconstructed map derived from the CWT2 analysis after threshold application.

The reconstructed map is obtained, in the space of wavelet coefficients, adding the wavelet coefficients of the scales selected from the wavelet variance map. It undergoes a threshold process to evidence the structures from the background. The threshold has been set as a function of the local mean and standard deviation of the reconstructed map, which depend both on the local meteorological conditions and the radar incidence angle.
The left panel of Figure 3 shows one of the ASAR WS images analyzed, while the right panel reports the reconstructed map after the application of the threshold: here the backscatter structures extracted by the analysis are in white and gray, and the background black. Only the cells with a major to minor axes ratio greater than two have been selected for wind retrieval, assuring they have a well defined asymmetric shape; the orientation of the cell's major axis is taken as the wind direction.
The texture of the reconstructed map typically produces a bimodal distribution of cells' direction, as seen in the left panel of Figure 4, which reports the direction's relative frequency distribution of the cells imaged in the right panel of Figure 3.

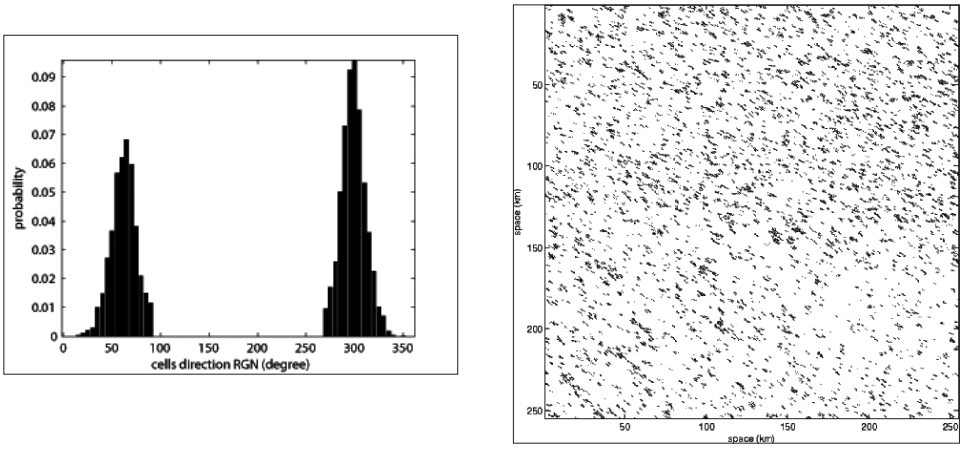

Figure 4 - Two steps to derive the aliased wind direction. Left panel: the relative frequency distribution of the cell directions derived from the reconstructed map. Right panel: the cells selected from the reconstructed map.

The cells directions Φ can cover only two quadrants, i.e. $270 \leq \Phi \leq 345°$ and $10 \leq \Phi \leq 90°$. The aliased wind orientation is taken as that corresponding to the most probable mode: in the example reported, the direction results $\Phi = 300°$ with a probability of 57 %, against a probability of 43 % to have $\Phi = 60°$.

The cells having directions around the most probable mode have been selected (see the right panel of Fig. 4), the others discarded. Note that this operation still preserves the possibility of wind direction variation around the most probable mode. When such cells are not present, no wind direction can be obtained. It happens frequently at the islands lee side and when the sea roughness is so weak that oceanographic features prevail on meteorological ones, and always when wind speed is below 3 m s^{-1} or so, because there is no sea roughness ignition at this wind regime [Pierson and Stacy, 1973]. The detection of the backscatter cells associated to the MABL permits also to get a description of its spatial characteristics, expressed in terms of cell's size and shape, as shown in Zecchetto and De Biasio [2002].

The dealiasing technique exploits the idea [Zecchetto et al., 1998; Zecchetto and De Biasio, 2002, 2008] that the modulation of the mean wind speed by the wind gustiness produces patches of sea surface roughness characterized by an asymmetric distribution of energy along the wind direction. The determination of the asymmetry inside the cells is the most delicate procedure: at present it is derived from the statistic of each cell maximum along the call major axis, but other statistical parameters are under study.

Once assessed the wind direction, the speed has been computed from the mean radar backscatter of the selected cells using the CMOD5 model [Hersbach et al., 2007]. This model has been derived essentially from ERS-2 scatterometer data with a spatial resolution of 50 km by 50 km, and its application to ASAR could be questionable, due both the possible mismatch between the absolute calibration of scatterometer and of ASAR and of the smaller size of the detected cells (O(1) km^2) with respect to the scatterometer resolution. This is an aspect which has to be investigated in future works.

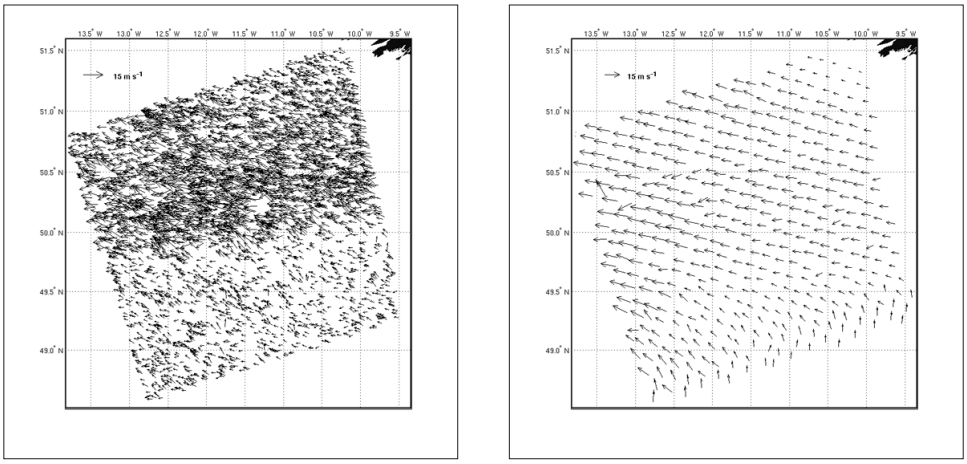

Figure 5 - The wind field. Left panel: wind field derived from the analysis of the image reported in the left panel of Figure 3 (20-JUN-2008 at 22:26 GMT). Right panel: the wind fields measured by QuikSCAT at 19:44 GMT (spatial resolution of 12.5 km by 12.5 km).

The wind field resulting after the processing of the images shown in the left panel of Figure 3 is reported in the left panel of Figure 5, while the right panel shows the wind fields as measured by QuikSCAT about two hours before. The ASAR derived wind field, with a spatial sampling uneven like the layout of the selected cells, shows a very detailed spatial structure, much more detailed than the 12.5 km by 12.5 km scatterometer winds.
The statistics of the two wind fields is shown in Figure 6. The wind speed distributions are, in this case, fairly different: there are much more SAR than scatterometer winds below 4 m s^{-1}, which makes the mean values different. However, the QuikSCAT winds appear in this case higher than those derived from SAR. On the contrary, the directions distributions result in agreement.
The nature of the differences of wind speed, possibly due to the mentioned problem of using the CMOD5 in small areas, to different spatial resolution of the ASAR derived winds with respect to those of scatterometer and to the different time of measurements, has to be investigated in future.

Conclusions

More three Envisat ASAR Wide Swath images are daily processed, since May 2008, using the methodology described in this paper. The images have been taken to cover the coastal areas of the region shown in Figure 2. Besides any specific scientific interest, the present aim of this on-line processing is to get a data set of ASAR images large enough for a statistical evaluation of the performances of the CWT2 method.
To accomplish this task it is necessary to have a large number of SAR derived wind fields co-located with the scatterometer winds. Since the collocation often fails due to the too large time gap between the pass time of Envisat and that of QuikSCAT and Metop, or it is limited by the partial overlapping of the scatterometer swath with the SAR frames. ERS-2 scatterometer data may be useful to overcome this problem, as this satellite flies in the same orbit of ENVISAT with a time delay of 30 minutes: their acquisition is planned in the near future activity.

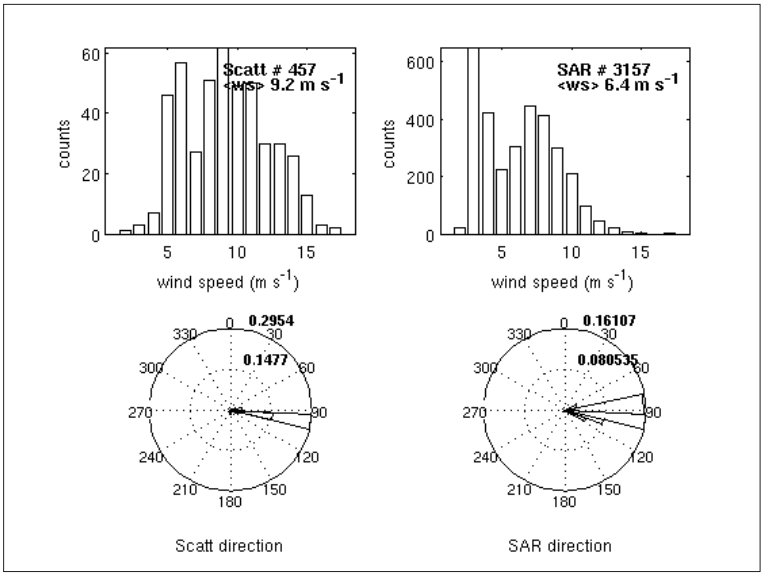

Figure 6 - The wind fields statistics. Top panels: wind speed distributions of QuikSCAT winds (left panel) and of ASAR derived winds (right panel). Bottom panels: direction distributions of QuikSCAT wind (left panel) and of ASAR derived wind directions (right panel).

Once available a large co located data set, it will be possible to estimate the differences of both the wind speed and direction provided by scatterometers and retrieved from SAR, and possibly to link the differences to the stability conditions of the air-sea interface. This is the necessary step in view of using the SAR derived wind fields in the coastal meteorology studies.

Acknowledgments

This work has been carried out on the framework of the Announcement of Opportunity for Envisat AO 464 and of the Project Start Up C1P.5404 of the European Space Agency. Scatterometer data at 25 km by 25 km of spatial resolution have been downloaded from the *KNMI ftp server* in the framework of the Ocean & Sea Ice Satellite Application Facility (`www.osi-saf.org`) of EUMETSAT (`www.eumetsat.org`). The Authors wish to thank the anonymous Referee for its remarks and suggestions.

References

Antoine J. P., Murenzi R. (2004) - *Two-Dimensional Wavelets and Their Relatives*. Cambridge University Press.

Beylkin G., Coifman R., Daubechies I., Mallat S., Meyer Y., Raphael L. (1992) - *Wavelets and their applications*. Jones and Barlett Publishers, Boston.

ESA (2002) - *Asar product handbook*. Technical report, European Space Agency, Paris, France.

ESA/Esrin and Telespazio (2006) - *Best, basic envisat sar toolbox, user guide*. Technical

Report version 4.0.5, European Space Agency.

Foufoula-Georgiou E., Kumar P. (1994) - *Wavelet in Geophysics, volume 4 of Wavelet analysis and its applications*. Academic Press, Inc., San Diego, CA.

Hersbach H., Stoffelen A., de Haan S. (2007) - *An improved scatterometer ocean geophysical model function: Cmod5*. Journal of Geophysical Research, 112: 5767-5780. doi:10.1029/2006jc003743.

JPL (2001) - *Quikscat science data product user's manual (ver. 2.1)*. Technical Report Publ. D-18053, 84 pp., Jet Propulsion Laboratory, Pasadena, USA.

Kaiser G. (1994) - *A friendly guide to wavelet*. Birkhauser, London.

Pierson W. J, Stacy R. A. (1973) - *The elevation, slope, and curvature spectra of the wind roughned sea surface*. Technical report, National Aereonautics and Space Administrations, Whashington D.C.

SAF (2007) - *ASCAT Wind Product User Manual*. Technical Report SAF/OSI/CDOP/KNMI/TEC/MA/126, Eumetsat, Darmstadt, Germany.

Torrence C., Compo G. (1998) - *A practical guide to wavelet analysis*. Bulletin of the American Meteorological Society, 79(1):61–78.

Zecchetto S., Trivero P., Fiscella B., Pavese P. (1998) - *Wind stress structure in the unstable marine surface layer detected by SAR*. Boundary Layer Meteorol., 86: 1–28.

Zecchetto S., De Biasio F. (2002) - *On shape, orientation and structure of atmospheric cells inside wind rolls in SAR images*. IEEE Trans. of Geoscience and Remote Sensing, 40(10):2257 – 2262.

Zecchetto S., De Biasio F. (2008) - *A wavelet based technique for sea wind extraction from SAR images*. IEEE Trans. of Geoscience and Remote Sensing.

Received 18/03/2009, accepted 12/05/2009.